eprints@whiterose.ac.uk
https://eprints.whiterose.ac.uk/

A Zebrafish Compound Screen Reveals Modulation of Neutrophil Reverse Migration as an Anti-Inflammatory Mechanism

Anne L. Robertson[1,2], Geoffrey R. Holmes[3], Aleksandra N. Bojarczuk[1], Joseph Burgon[1], Catherine A. Loynes[1,2], Myriam Chimen[4], Amy K. Sawtell[5], Bashar Hamza[6], Joseph Willson[2], Sarah R. Walmsley[2], Sean R. Anderson[3], Mark C. Coles[5], Stuart N. Farrow[7], Roberto Solari[8], Simon Jones[9], Lynne R. Prince[2], Daniel Irimia[6], G. Ed Rainger[4], Visakan Kadirkamanathan[3], Moira K. B. Whyte[1,2], and Stephen A. Renshaw[1,2,*]

[1]Medical Research Council Centre for Developmental and Biomedical Genetics, University of Sheffield, Sheffield S10 2TN, UK

[2]Department of Infection and Immunity, University of Sheffield, Sheffield S10 2RX, UK

[3]Department of Automatic Control and Systems Engineering, University of Sheffield, Sheffield S1 3JD, UK

[4]Centre for Cardiovascular Sciences, School of Clinical and Experimental Medicine, University of Birmingham, Birmingham B15 2TT, UK

[5]Centre for Immunology and Infection, Department of Biology, University of York, York YO10 5DD, UK

[6]Department of Surgery, Massachusetts General Hospital, Harvard Medical School, Boston, MA 02114, USA

[7]Respiratory Therapy Area, GlaxoSmithKline, Stevenage SG1 2NY, UK

[8]National Heart and Lung Institute, Imperial College London, Norfolk Place, London W2 1PG, UK

[9]Department of Chemistry, University of Sheffield, Sheffield S3 7HF, UK

*Corresponding author. s.a.renshaw@sheffield.ac.uk.

SUPPLEMENTARY MATERIALS

www.sciencetranslationalmedicine.org/cgi/content/full/6/225/225ra29/DC1

Materials and Methods

Fig. S1. Positive hit compounds significantly reduce neutrophil numbers at 12 hpi to accelerate inflammation resolution.

Fig. S2. A subset of the positive hit compounds inhibits neutrophil recruitment.

Fig. S3. Positive hit compounds have no significant effects on total neutrophil number.

Fig. S4. Cryptotanshinone accelerates neutrophil apoptosis in vitro and overrides GM-CSF–induced survival.

Fig. S5. Inflammation resolution is delayed in the presence of dominant-active *hif-1αb*.

Fig. S6. Tanshinone IIA does not affect neutrophil reverse transmigration across endothelial monolayers in vitro.

Fig. S7. Tanshinone IIA does not alter cytokine production in stimulated monocytes.

Abstract

Diseases of failed inflammation resolution are common and largely incurable. Therapeutic induction of inflammation resolution is an attractive strategy to bring about healing without increasing susceptibility to infection. However, therapeutic targeting of inflammation resolution has been hampered by a lack of understanding of the underlying molecular controls. To address this drug development challenge, we developed an in vivo screen for proresolution therapeutics in a transgenic zebrafish model. Inflammation induced by sterile tissue injury was assessed for accelerated resolution in the presence of a library of known compounds. Of the molecules with proresolution activity, tanshinone IIA, derived from a Chinese medicinal herb, potently induced inflammation resolution in vivo both by induction of neutrophil apoptosis and by promoting reverse migration of neutrophils. Tanshinone IIA blocked proinflammatory signals in vivo, and its effects are conserved in human neutrophils, supporting a potential role in treating human inflammation and providing compelling evidence of the translational potential of this screening strategy.

INTRODUCTION

Resolution of inflammation is an active and regulated process accompanying the elimination of infection and repair of damaged tissue, which is critical for the maintenance of tissue homeostasis. An essential step toward achieving successful inflammation resolution is the clearance of tissue neutrophils (1). Neutrophils are highly evolved for host defense and destroy foreign pathogens through phagocytosis, degranulation, and the formation of reactive oxygen species and neutrophil extracellular traps (2). These powerful effector functions must be limited to avoid persistent inflammation; this can be achieved by either the well-characterized process of neutrophil apoptosis or the more recently reported exit of neutrophils from inflammatory sites, best described as " reverse migration" (3–6).

Dysregulation of the mechanisms governing neutrophil clearance is associated with the pathogenesis of chronic inflammatory diseases (2). Many such diseases, particularly those dominated by persistent neutrophilic inflammation such as chronic obstructive pulmonary disease, respond poorly to conventional treatments. Uncovering new mechanisms by which inflammation resolution can be therapeutically enhanced is key to developing more effective therapies for such conditions. Inflammation resolution can be accelerated by induction of neutrophil apoptosis, for example, by inhibition of cyclin-dependent kinases (7), but it is not yet clear how such an approach can be balanced against the essential host defense functions of the neutrophil.

Proresolution therapies are an attractive strategy with the potential to remove unwanted neutrophils while leaving host-protective functions intact. Current approaches replicating endogenous proresolution signals are showing promise as potential therapeutics (8–11). Drug discovery programs in this area are, however, impeded by a lack of understanding of the molecular events controlling inflammation resolution. Recent advances using zebrafish for in vivo chemical biology have shown how a phenotype-based approach can yield new drug candidates and drug targets without a detailed understanding of the underlying molecular mechanisms (12–14). Inflammation resolution is an ideal physiological process

for dissection using chemical biology approaches, and to this end, we developed an in vivo chemical genetic screen using our neutrophil-specific *Tg(mpx:GFP)i114* zebrafish line (15).

In this investigation, we build on our own pilot data, and that from others (16–18), to describe a new semiautomated platform for high-content drug discovery. This approach enables rapid and robust chemical genetic screening and, importantly, has led to the identification of a compound, tanshinone IIA, derived from a Chinese medicinal herb and having profound anti-inflammatory effects. We show that this compound accelerates inflammation resolution in the presence and absence of proinflammatory stimuli in both zebrafish and human systems by accelerating the parallel mechanisms of reverse migration and neutrophil apoptosis.

RESULTS

A zebrafish chemical genetic screen identifies accelerators of inflammation resolution

We have previously described a preliminary, proof-of-principle compound screen (16) in which we identified 12 compounds that accelerated inflammation resolution by reducing neutrophil numbers without affecting preceding recruitment in our zebrafish tail fin injury model. Half of these compounds had known anti-inflammatory activity, demonstrating the potential of this unbiased screening approach. We optimized and partially automated our screening assay using the Phenosight High-Content Screening System (Ash Biotech), a custom-built imaging platform enabling rapid data acquisition and assessment of drug efficacy and toxicity. By injuring *mpx*:GFP larvae at 3 days post-fertilization (dpf), we induce a reproducible and robust inflammatory response, quantifiable by neutrophil number or by green fluorescence localized to the injury region, which can be tracked over time (Fig. 1A). To focus our efforts on compounds influencing inflammation resolution and to minimize identification of generalized inhibitors of recruitment, we exposed injured larvae to compounds from 4 hours post-injury (hpi), a time point when high numbers of neutrophils have been recruited to the wound site, until 12 hpi when inflammation resolution is only partially complete in controls (15). Larvae are imaged on the Phenosight High-Content Screening System, enabling identification of those larvae with less inflammation (Fig. 1A, lower panel), as described in Materials and Methods. We chose the Spectrum Collection of 2000 compounds because this included well-characterized U.S. Food and Drug Administration–approved drugs, natural products, and defined pathway inhibitors. Screening this library identified 21 reproducible positive hits (Fig. 1, B and C), from which we selected the 9 most effective compounds for further study. The compounds selected were those that scored highest, that is, had the fewest neutrophils remaining at the wound compared with untreated controls by manual scoring and that did not appear to cause toxicity, as evidenced by death or morphological abnormality.

For each of the positive " hit" compounds, we studied their activity on neutrophil behavior in vivo in three assays. To test recruitment, we treated larvae immediately after tail fin injury and counted the number of neutrophils at the site of injury after 6 hours. To test for effects on inflammation resolution, we treated larvae from 6 to 12 hpi. We also performed a whole-body total neutrophil count in uninjured fish to control for developmental changes caused by drug treatment. To understand the effects of our compounds on inflammation resolution, we

compared their activity in these assays to a panel of well-characterized compounds containing known inhibitors of key inflammatory signaling pathway components including phosphatidylinositol 3-kinase (PI3K), mitogen-activated protein kinase (MAPK), and phosphodiesterase 4 (PDE4) (19–25). All of our hits significantly reduced neutrophil numbers in assays of inflammation resolution in a concentration-dependent manner (fig. S1), and a subset of these also had some effect on neutrophil recruitment (fig. S2). None of our lead compounds significantly altered total neutrophil numbers compared to the vehicle control (fig. S3). To compare our compounds to the effects of known pathway inhibitors, we used hierarchical cluster analysis (Fig. 1D).Most of our positive hits formed a group clustered together, distinct to the known inhibitors of inflammatory signaling pathways. These compounds demonstrated potent proresolution activity with only moderate effects on neutrophil recruitment. As anticipated, known anti-inflammatory compounds predominantly affected recruitment. Of particular interest, two of the compounds that we identified, tanshinone IIA and cryptotanshinone, shared close structural similarity (Fig. 1E). These diterpine quinones are both natural extracts from *Salvia miltiorrhiza*, a Chinese medicinal herb traditionally used to treat cardiovascular disorders (26). Tanshinone IIA is known to have anti-inflammatory activity and has protective effects against lipopolysaccharide (LPS)–induced lung injury in mammalian systems (27, 28).However, there is little known about the mechanisms involved. We explored the activity of tanshinone IIA in our zebrafish model to determine whether it had any specific effects on neutrophilic inflammation.

Tanshinone IIA accelerates resolution of inflammation in vivo without significantly affecting neutrophil recruitment

Tanshinone IIA is a powerful accelerator of inflammation resolution, significantly reducing neutrophil numbers at 12 hpi in a concentration-dependent manner (Fig. 2A). We observed no change in total neutrophil numbers in tanshinone IIA–treated larvae, suggesting that the compound acts specifically on activated neutrophils participating in the inflammatory response to drive resolution in acute inflammation (Fig. 2B).We found a small increase in neutrophil apoptosis at the site of tissue injury (Fig. 2, C to E), indicating that this mechanism may partly explain the proresolution activity of tanshinone IIA. We also explored the effects of tanshinone IIA on the initial phase of inflammation. At 6 hpi, tanshinone IIA did not significantly reduce the number of neutrophils recruited to the site of injury, although there was a trend toward fewer neutrophils at the wound at the highest concentrations tested (Fig. 3A). To further examine the effect of tanshinone IIA on specific aspects of neutrophil migratory behavior, we tracked neutrophils for the first hour after tail fin transection in *mpx*:GFP larvae pretreated with either tanshinone IIA or dimethyl sulfoxide (DMSO) for 2 hours. Analysis revealed no differences in neutrophil speed (distance traveled per second), displacement (linear distance between the start and end of a neutrophil track), or meandering index (total path length divided by displacement) (29) in tanshinone IIA–treated larvae compared to the DMSO vehicle control (Fig. 3, B to D). Neutrophil bearing (angle of movement toward the wound) also remained unchanged, which suggested that the cells remained able to respond to the chemotactic gradient in the presence of tanshinone IIA.

Tanshinone IIA overrides human neutrophil survival signals

Neutrophil survival signals are thought to be a major mechanism driving prolongation of inflammation in pathological settings (30, 31). The acceleration of inflammation resolution observed in the zebrafish model is consistent with a role for tanshinone IIA in overriding survival signaling, allowing neutrophil apoptosis to proceed. To test this hypothesis directly, while simultaneously extending our findings into a human system, we tested the effect of tanshinone IIA on freshly isolated human neutrophils. Tanshinone IIA caused a significant increase in apoptosis after 8 hours in culture, when assessed by both morphology (Fig. 4A) and annexin V/propidium iodide (PI) staining (Fig. 4B). With the addition of either granulocyte-macrophage colony-stimulating factor (GM-CSF) or dimethyloxalylglycine (DMOG), stimuli that promote neutrophil longevity (30, 32), there was a complete loss of stimulus-induced neutrophil survival in the presence of tanshinone IIA (Fig. 4, C and D). The closely related molecule cryptotanshinone was also found to accelerate human neutrophil apoptosis and override GMCSF–induced neutrophil survival (fig. S4). These data support the potential of tanshinone IIA as a therapeutic for human inflammatory disease.

Tanshinone IIA accelerates inflammation resolution in vivo via an unsuspected mechanism

As has been shown in a range of in vivo models (16, 29), visible examples of neutrophil apoptosis during inflammation resolution were scarce in our zebrafish model. Although this could relate to the short half-life of apoptotic neutrophils within inflamed tissues where patrolling macrophages rapidly phagocytose such cells (33), we speculated that the profound proresolution effect of tanshinone IIA might be mediated via an additional effect on reverse migration. Reverse migration of neutrophils away from sites of injury has been observed in zebrafish by a number of research groups (4, 29, 34, 35), and related phenomena have also been reported to occur in mammalian systems (3, 6, 36). To assay for reverse migration specifically of neutrophils, we generated a new transgenic line where a bacterial artificial chromosome (BAC) was targeted with Gal4-VP16. This line recapitulates expression of our existing *mpx:*GFP line and expresses Kaede specifically in neutrophils when crossed to the UAS:Kaede line. Using *mpx*/Kaede double transgenic larvae from this new line, we initiated the inflammatory response as before and then allowed inflammation to proceed. At 6 hpi, we photoconverted neutrophils at the injury site (Fig. 5A) and followed their behavior during the resolution phase of the inflammatory response, measuring the numbers of neutrophils that migrated away from the site of injury over time, as previously described (29). Strikingly, we found that neutrophils in tanshinone IIA–treated larvae moved away from the site of injury more quickly than did cells in DMSO control larvae (Fig. 5, A and B). We also found that tanshinone IIA accelerated inflammation resolution, even in the presence of activated hypoxia-inducible factor (Hif) signaling, which we have previously shown to delay inflammation resolution (fig. S5) (29). Similar to our earlier experiments, tanshinone IIA reduced neutrophil numbers at the wound at 12 hpi in larvae injected with dominant-active *hif-1αb* RNA (Fig. 5C), by an increase in neutrophil reverse migration (Fig. 5D). These data indicate that tanshinone IIA can override proinflammatory signaling pathways during inflammation resolution in vivo.

Our results suggest that tanshinone IIA exerts its predominant proresolution effect in vivo by accelerating the endogenous reverse migratory behavior of neutrophils, thus promoting neutrophil clearance from the wound. This appears to require a complex tissue environment because currently available in vitro models of human neutrophil reverse transmigration through endothelial monolayers (3, 37) do not show enhanced reverse migration with tanshinone IIA (fig. S6). In addition, tanshinone IIA did not affect cytokine release from stimulated monocytes in vitro (fig. S7), suggesting that it is most likely that tanshinone IIA directly regulates the neutrophil, rather than altering the function of an intermediate cell type. We have shown that it is possible to drive inflammation resolution by pharmacologically enhancing neutrophil reverse migration, and this, in combination with the apoptosis-inducing properties of tanshinone IIA, appears to account for its highly significant proresolution activity in our assays.

Tanshinone IIA does not establish a fugetactic signal to drive inflammation resolution

In zebrafish, migration of neutrophils away from wounds was initially described as " retrograde chemotaxis," in which neutrophils migrated back into the vasculature in an active, or directed, manner (4, 35). More recently, computational modeling of the migration dynamics of neutrophils undergoing reverse migration after tail fin transection has suggested that this process may be more accurately described as a process of nondirectional redistribution, whereby neutrophils redistribute in tissues as a consequence of essentially random motion (38, 39). We use the term reverse migration here because this simply describes our observation and does not convey a mechanistic explanation. Two distinct mechanisms might explain the ability of tanshinone IIA to drive inflammation resolution by reverse migration in vivo: Either tanshinone IIA causes an acceleration of nondirectional redistribution of neutrophils by altering response to existing gradients, or it acts by establishing a fugetactic gradient that repels neutrophils from the wound. To determine which explanation is most likely, we applied two previously described analytical approaches. First, we considered the mean squared distance of photoconverted neutrophils from the wound (38) (Fig. 6A). When plotted against time, mean squared distance of photoconverted neutrophils from the wound has a linear relationship to time. This is true in the case of both tanshinone IIA and the DMSO control, suggesting that the migration occurs in a random manner without any fugetactic drift. However, with the addition of tanshinone IIA, the fitted linear model has a steeper gradient, indicating that the process of reverse migration is accelerated.

To confirm these findings, a second approach (39), which uses approximate Bayesian computation (40), was applied to predict the best model from a diffusion-only model (nondirectional redistribution) versus a drift diffusion model (fugetaxis). In the vast majority of simulations, the effect of tanshinone IIA was best described by nondirectional redistribution (Fig. 6, B to E), with the diffusivity of neutrophils about double that in the control larvae (Fig. 6C). Diffusivity is a measure of how quickly randomly moving cells will disperse away from each other if they are initially grouped together, which is related to both the speed at which they move and the direction of their migration paths. The increase in diffusivity caused by tanshinone IIA reflects the difference observed in Fig. 6A. We found that this increase in diffusivity was not simply due to increased neutrophil speed in the

presence of tanshinone IIA, because when individual neutrophil tracks were analyzed, there were no differences between neutrophils from tanshinone IIA– or DMSO-treated larvae (Fig. 6, F and G).

DISCUSSION

A rapid and simple in vivo system for testing the ability of drugs and other chemical entities to drive inflammation resolution has a number of advantages over alternative approaches. A model with a fully functioning immune system enables the identification of mechanisms involving the interactions of different cell types and can be used to reveal unanticipated counterregulatory effects, which could not be identified in vitro. In addition, by administering the drug to an established inflammatory lesion, it is possible to dissect the effects of compounds on neutrophil recruitment from those on resolution, to identify specific proresolution agents.

As proof of principle, we show how tanshinone IIA was identified and functionally characterized as a proresolution molecule. This compound acts on both zebrafish and human neutrophils to increase levels of apoptosis. Moreover, it can promote reverse migration of neutrophils, uncovering a potential therapeutic mechanism to drive inflammation resolution. We have previously shown that an increase in hypoxic signaling, via stabilization of Hif-1α, can modulate reverse migration by retaining neutrophils at inflammatory sites (29). Tanshinone IIA has the opposing effect and can overcome the effect of Hif-1α stabilization to promote reverse migration. Other pharmacological drivers of inflammation resolution are also reported to override neutrophil survival factors (41), and this activity may be important for novel proresolution therapeutics.

Tanshinone IIA is effective in a number of models of inflammation (27, 42) including LPS-induced lung injury in the mouse (28). These effects have not been attributed to actions on a single cell type but are suggested to be dependent on inhibition of nuclear factor κB (NF-κB). This is supported by evidence from in vitro systems where the downstream effects of this inhibition have been illustrated by reduced expression of adhesion molecules and reduced production of nitric oxide and prostaglandins in macrophage cell lines (43–45). Tanshinones have also been implicated in the inhibition of other transcription factors such as activating protein 1 (AP-1) and signal transducer and activator of transcription 1 (STAT1) (46, 47). We have not yet identified the molecular events downstream of tanshinone IIA treatment in neutrophils and how these might regulate reverse migration.

The current study has a number of limitations. Although we have partially automated our assay, tail fin injury still requires a significant manual intervention, which limits throughput. Efficacious compounds may be missed because of inefficient larval penetration, although this may be balanced by the increased value of positive hits identified in this way. Finally, we would like to demonstrate therapeutic modulation of neutrophil reverse migration in man with tanshinone IIA, but this is currently not possible with existing experimental approaches.

The best-described mechanism by which neutrophils are removed from sites of inflammation is apoptosis, a controlled process that prevents excessive release of proinflammatory and histotoxic neutrophil contents (1, 2) and modulates the inflammatory potential of phagocytic macrophages (2). The biochemical pathways affecting neutrophil life span, particularly those activated by endogenous survival signals such as GM-CSF (30) and hypoxia (32), though complex, are reasonably well understood, and pharmacological inhibition of downstream signaling pathways has yielded some therapeutic benefit in mammalian systems (2, 48). Proresolution strategies targeting apoptosis have shown great promise, by targeting either cyclin-dependent kinases or, more recently, serum- and glucocorticoid-regulated kinase (SGK) (41, 49). We have now identified another pharmacological modulator of neutrophil survival, tanshinone IIA, which has the additional effect of accelerating reverse migration—likely to be the main mechanism of inflammation resolution in this system. Potential interaction of tanshinone IIA with endogenous regulators of inflammation resolution is an interesting question for future research.

A number of lines of evidence now suggest that viable neutrophils can leave sites of inflammation, including by reverse migration. Studies in human neutrophils revealed that reverse transmigrated neutrophils display a unique cell surface receptor phenotype with elevated expression of CD11b and ICAM-1 and reduced expression of CXCR1 (3). A similar phenomenon, termed retrotaxis, has more recently been described, in which human neutrophils migrate away from chemotactic gradients in microfluidic systems (50). In mice, neutrophils have been reported to undergo reverse transendothelial migration more frequently after genetic or pharmacological inhibition of the junctional adhesion molecule JAM-C, and these neutrophils also have distinctive elevated expression of ICAM-1 (6). The proinflammatory potential of these cells is in contrast to the proresolution effects of tanshinone IIA, and this difference will require resolution in future studies. Reverse migration can be visualized more readily and in real time using transparent zebrafish larvae in which large numbers of fluorescently labeled neutrophils are observed to leave a wound site (4, 29, 34, 35), making this an ideal model organism in which to illuminate the mechanisms involved. Here, we provide evidence to show that reverse migration can be pharmacologically promoted to drive inflammation resolution in vivo. The relative importance of reverse migration versus neutrophil apoptosis during inflammation resolution in humans remains to be determined. Our data indicate that both processes are targeted by tanshinone IIA, broadening the appeal of this compound as a potential therapeutic.

Our data strongly suggest that reverse migration is a process of non-directional redistribution rather than directed fugetaxis (38, 39). The data presented here suggest that tanshinone IIA accelerates the loss of sensitivity of neutrophils to their chemotactic environment rather than driving neutrophils away from inflammatory sites by directed programs of migration. The large increase in diffusivity of tanshinone IIA–activated neutrophils, combined with lack of active drift away from the wound, suggests that tanshinone IIA acts to accelerate the loss of sensitivity to the neutrophils' chemotactic environment. This process is entirely different from a ligand-based fugetaxis mechanism, suggesting that future studies must look for internal mechanisms within the neutrophil for the defining events in inflammation resolution. This result also underlines the value of

stochastic computational modeling of cell migration in aiding understanding of the underlying biological mechanisms.

These studies establish the value of tanshinone IIA in inhibiting survival signals in human neutrophils. Furthermore, the safety and efficacy of tanshinone IIA in rodent models have been previously established, and there is clinical experience of the molecule in its unprocessed form in humans. Experimental medicine studies in humans will now be necessary as a prelude to a larger-scale clinical trial.

In summary, this study demonstrates the utility of zebrafish models for chemical screens for activity specifically in the proresolution phase of inflammation and describes the functional characterization of a key hit from a compound library screen. This approach has illustrated its value by uncovering a compound that offers both potential therapeutic utility and novel insights into the biology of inflammation resolution.

MATERIALS AND METHODS

Study design

The initial objective of our study was to identify novel accelerators of inflammation resolution via an unbiased chemical screening approach. Using *Tg(mpx:GFP)i114* zebrafish larvae as an in vivo model, we investigated the effect of screening compounds on neutrophil numbers during the resolution phase of inflammation. Larvae were injured at 3 dpf by complete transection of the caudal fin with a microscalpel. Because of their inherent natural variability, a proportion of larvae recruit very few neutrophils to the site of injury. Therefore, to minimize the detection of false positives, we selected larvae that recruited high numbers of neutrophils to the wound by 4 hpi. Larvae from this group were then randomly dispensed into wells containing screening compounds, at a density of three larvae per well. Larvae were incubated with compounds until 12 hpi, a time point at which neutrophil numbers remain relatively high in negative control larvae and compounds causing accelerated resolution can be reliably identified (16). For the primary screen, each compound was tested on two independent occasions (six larvae in total). Larvae were imaged for analysis by manual scoring, and a mean score of 1.5 was used as the threshold for positive hit selection. Positive hits from the primary screen were retested on four independent occasions (12 larvae in total). In all cases, control wells were blinded, and the identity of the screening compounds was unknown until after analysis was performed.

Reagents

Drug screening was performed on the Spectrum Collection (2010 version; MicroSource Discovery Systems). All compounds were dissolved in DMSO, such that 1% DMSO was used as a negative control (Sigma-Aldrich). Reagents used as positive controls were an inhibitor of SGK, GSK650394 (Tocris Bioscience), at 10 μM and the c-Jun N-terminal kinase inhibitor SP600125 (Sigma-Aldrich) at 30 μM. The panel of known anti-inflammatory compounds was obtained from GlaxoSmithKline. Tanshinone IIA and cryptotanshinone were obtained from Sigma-Aldrich, DMOG was from Enzo Life Sciences, and GM-CSF was from PeproTech.

Zebrafish husbandry and assays

Zebrafish were raised and maintained according to standard protocols (51) in UK Home Office–approved aquaria in the Medical Research Council (MRC) Centre for Developmental and Biomedical Genetics at the University of Sheffield. The neutrophil-specific zebrafish line *Tg(mpx:GFP)i114*, referred to as *mpx*:GFP, was used for all drug screening, inflammation assays, and neutrophil tracking assays at 3 dpf as previously described (29). For resolution assays, larvae that recruited high numbers of neutrophils to the wound (about 30 cells) were selected for compound treatment at 6 hpi, and neutrophil counts were performed at 12 hpi. In all inflammation assays, tail fins were transected at the region indicated in Fig. 1A, and neutrophils in the region posterior to the circulatory loop were counted at the appropriate time point. Compounds were used at the doses indicated in each figure. To assess total neutrophil number, uninjured larvae were incubated with compounds for 24 hours, mounted in 1% low-melting point agarose (Sigma-Aldrich), and imaged on an Eclipse TE2000-U inverted compound fluorescence microscope (Nikon) at ×2 magnification. Total neutrophil numbers were quantified with ImageJ.

Drug screening was performed with the Phenosight High-Content Screening System (Ash Biotech). Larvae that recruited high numbers of neutrophils to the wound by 4 hpi (about 25 to 30 cells) were selected and arrayed into 96-well plates containing compounds from the Spectrum Collection at 25 μM. Compounds were tested alongside untreated controls, 1% DMSO vehicle controls, and either 10 μMGSK650394 or 30 μMSP600125 as a positive control. At 12 hpi, plates were scanned on the Phenosight High-Content plate reader. Images generated were analyzed by manual scoring, in which each well containing three larvae was assigned a score between 0 and 3, corresponding to the number of larvae within the well with a reduced number of neutrophils at the site of injury compared to the vehicle control. Neutrophil apoptosis was measured in paraformaldehyde-fixed larvae after TSA staining (TSA Plus, PerkinElmer) to label neutrophil myeloperoxidase with green fluorescent protein (GFP), along with ApopTag Red In Situ Apoptosis Detection Kit (TUNEL) (Millipore Corp.) to label apoptotic cells, as previously described (29). The total neutrophil number at the wound (TSA-positive) and number of apoptotic neutrophils (dual TSA/TUNEL-positive) were quantified with Volocity to calculate the percentage of neutrophil apoptosis. Reverse migration assays were performed following established methods (29, 39), with *Tg(mpx:Gal4);Tg(UAS:Kaede)i222* larvae, referred to as *mpx*/Kaede.

Overexpression of dominant-active hif-1αb RNA

The dominant-active form of *hif-1αb* was generated as described previously (29). RNA was transcribed (mMESSAGE mMACHINE, Ambion, Invitrogen) and injected into *mpx*/Kaede embryos at the one-cell stage, with established methods (51). Reverse migration experiments were performed at 2 dpf as described (29).

Human neutrophil apoptosis assays

Peripheral blood neutrophils were purified as described previously (52), in accordance with the South Sheffield Research Ethics Committee (reference number: STH13927). Neutrophils were cultured for 8 hours, with DMSO control or tanshinone IIA at the dose indicated, and 100 μM DMOG or GM-CSF (0.01 μg/ml), as indicated. Rates of neutrophil apoptosis based

on morphology were counted blindly on cytospins stained with Quick-Diff (Gentaur). For each condition, two cytospins were acquired with a cytocentrifuge at 2000 rpm for 2 min. After fixing with 100% MeOH, cytospins were stained with Reastain Quick-Diff (Gentaur). With an upright microscope (Zeiss) at ×100 magnification, neutrophils were allocated as either apoptotic or nonapoptotic based on morphology. A total of 600 neutrophils were counted per condition (300 per cytospin) to calculate percentage neutrophil apoptosis. To assess neutrophil apoptosis by flow cytometry, neutrophils were cultured as described for morphology assays and then centrifuged at 3000 rpm for 3 min. Neutrophil pellets were resuspended in annexin V binding buffer and stained with Alexa Fluor 647 annexin V, followed by PI solution (BD Biosciences). Samples were run in duplicate on a FACSArray flow cytometer, and 10,000 events were captured within the neutrophil gate each time. Percentages of annexin V– and PI-positive neutrophils were analyzed with FlowJo.

Mathematical modeling of inflammation resolution data

Modeling was applied to the data presented in Fig. 5A, which represents about 25 neutrophils from each larva (total of about 600 neutrophils per condition). The coordinates of each neutrophil were identified with Volocity and the distance from the wound squared to calculate the mean squared distance at each time point, as described (38). A simulation-based ABC-SMC approach was used for estimation and comparison between pure diffusion and drift diffusion models, as described in (39, 40). At the first iteration, a population of models was chosen at random from the two possible models. For each chosen model, diffusivity and drift parameters were selected from a previous range of plausible values. The model was then simulated to yield observations that could be compared to the experimental observations, and the difference between these observation sets was calculated. If the difference was less than a chosen threshold, then the model was kept as a sample from the posterior distribution. Subsequent iterations chose model and parameter sets from those accepted in the previous iteration subject to small perturbations, and the error threshold was reduced. By the end of the process, only model/parameter samples that gave an output close to the experimental observations remained.

Statistical analysis

Throughout figures, data shown are means ± SEM of all data points from individual animals. Data were analyzed with unpaired, two-tailed *t* tests for comparisons between two groups and one-way ANOVA (with appropriate post-test adjustment) for other data (Prism 5.0; GraphPad Software). Hierarchical cluster analysis was performed on normalized data with Cluster 3.0 (developed by M. de Hoon), with Pearson uncentered correlation and an average linkage clustering method. Results generated are displayed with Java TreeView (developed by A. Saldanha). Both programs were downloaded from http://www.eisenlab.org/eisen/?page_id=42. Recruitment and resolution assay data were normalized by expressing as a percentage of the effect of the positive control SP600125, and total neutrophil number assay data were expressed as the percentage change from the DMSO control.

Supplementary Material

Refer to Web version on PubMed Central for supplementary material.

Acknowledgments

REFERENCES AND NOTES

1. Serhan CN, Savill J. Resolution of inflammation: The beginning programs the end. Nat. Immunol. 2005; 6:1191–1197. [PubMed: 16369558]

2. Fox S, Leitch AE, Duffin R, Haslett C, Rossi AG. Neutrophil apoptosis: Relevance to the innate immune response and inflammatory disease. J. Innate Immun. 2010; 2:216–227. [PubMed: 20375550]

3. Buckley CD, Ross EA, McGettrick HM, Osborne CE, Haworth O, Schmutz C, Stone P, Salmon M, Matharu N, Vohra RK, Nash GB, Rainger GE. Identification of a phenotypically and functionally distinct population of long-lived neutrophils in a model of reverse endothelial migration. J. Leukoc. Biol. 2006; 79:303–311. [PubMed: 16330528]

4. Mathias JR, Perrin BJ, Liu TX, Kanki J, Look AT, Huttenlocher A. Resolution of inflammation by retrograde chemotaxis of neutrophils in transgenic zebrafish. J. Leukoc. Biol. 2006; 80:1281–1288. [PubMed: 16963624]

5. Uller L, Persson CGA, Erjefält JS. Resolution of airway disease: Removal of inflammatory cells through apoptosis, egression or both? Trends Pharmacol. Sci. 2006; 27:461–466. [PubMed: 16876880]

6. Woodfin A, Voisin MB, Beyrau M, Colom B, Caille D, Diapouli F, Nash G, Chavakis T, Albelda SM, Meda P, Imhof BA, Nourshargh S. The junctional adhesion molecule JAM-C regulates polarized transendothelial migration of neutrophils in vivo. Nat. Immunol. 2011; 12:761–769. [PubMed: 21706006]

7. Rossi AG, Sawatzky DA, Walker A, Ward C, Sheldrake TA, Riley NA, Caldicott A, Martinez-Losa M, Walker TR, Duffin R, Gray M, Crescenzi E, Martin MC, Brady HJ, Savill JS, Dransfield I, Haslett C. Cyclin-dependent kinase inhibitors enhance the resolution of inflammation by promoting inflammatory cell apoptosis. Nat. Med. 2006; 12:1056–1064. [PubMed: 16951685]

8. Schwab JM, Chiang N, Arita M, Serhan CN. Resolvin E1 and protectin D1 activate inflammation-resolution programmes. Nature. 2007; 447:869–874. [PubMed: 17568749]

9. Uddin M, Levy BD. Resolvins: Natural agonists for resolution of pulmonary inflammation. Prog. Lipid Res. 2011; 50:75–88. [PubMed: 20887750]

10. Dalli J, Winkler JW, Colas RA, Arnardottir H, Cheng CYC, Chiang N, Petasis NA, Serhan CN. Resolvin D3 and aspirin-triggered resolvin D3 are potent immunoresolvents. Chem. Biol. 2013; 20:188–201. [PubMed: 23438748]

11. Eickmeier O, Seki H, Haworth O, Hilberath JN, Gao F, Uddin M, Croze RH, Carlo T, Pfeffer MA, Levy BD. Aspirin-triggered resolvin D1 reduces mucosal inflammation and promotes resolution in a murine model of acute lung injury. Mucosal Immunol. 2013; 6:256–266. [PubMed: 22785226]

12. North TE, Goessling W, Walkley CR, Lengerke C, Kopani KR, Lord AM, Weber GJ, Bowman TV, Jang I, Grosser T, FitzGerald GA, Daley GQ, Orkin SH, Zon LI. Prostaglandin E2 regulates vertebrate haematopoietic stem cell homeostasis. Nature. 2007; 447:1007–1011. [PubMed: 17581586]

13. Yu PB, Hong CC, Sachidanandan C, Babitt JL, Deng DY, Hoyng SA, Lin HY, Bloch KD, Peterson RT. Dorsomorphin inhibits BMP signals required for embryogenesis and iron metabolism. Nat. Chem. Biol. 2008; 4:33–41. [PubMed: 18026094]

14. Laggner C, Kokel D, Setola V, Tolia A, Lin H, Irwin JJ, Keiser MJ, Cheung CYJ, Minor DLJ, Roth BL, Peterson RT, Shoichet BK. Chemical informatics and target identification in a zebrafish phenotypic screen. Nat. Chem. Biol. 2011; 8:144–146. [PubMed: 22179068]

15. Renshaw SA, Loynes CA, Trushell DMI, Elworthy S, Ingham PW, Whyte MKB. A transgenic zebrafish model of neutrophilic inflammation. Blood. 2006; 108:3976–3978. [PubMed: 16926288]

16. Loynes CA, Martin JS, Robertson AL, Trushell DMI, Ingham PW, Whyte MKB, Renshaw SA. Pivotal Advance: Pharmacological manipulation of inflammation resolution during spontaneously resolving tissue neutrophilia in the zebrafish. J. Leukoc. Biol. 2010; 87:203–212. [PubMed: 19850882]

17. d' Alençon CA, Peña OA, Wittmann C, Gallardo VE, Jones RA, Loosli F, Liebel U, Grabher C, Allende ML. A high-throughput chemically induced inflammation assay in zebrafish. BMC Biol. 2010; 8:151. [PubMed: 21176202]

18. Wang X, Robertson AL, Li J, Chai RJ, Haishan W, Sadiku P, Ogryzko NV, Everett M, Yoganathan K, Luo HR, Renshaw SA, Ingham PW. Inhibitors of neutrophil recruitment identified using transgenic zebrafish to screen a natural product library. Dis. Model. Mech. 2014; 7:163–169. [PubMed: 24291762]

19. Friesen RW, Ducharme Y, Ball RG, Blouin M, Boulet L, Côté B, Frenette R, Girard M, Guay D, Huang Z, Jones TR, Laliberté F, Lynch JJ, Mancini J, Martins E, Masson P, Muise E, Pon DJ, Siegl PKS, Styhler A, Tsou NN, Turner MJ, Young RN, Girard Y. Optimization of a tertiary alcohol series of phosphodiesterase-4 (PDE4) inhibitors: Structure–activity relationship related to PDE4 inhibition and human ether-a-go-go related gene potassium channel binding affinity. J. Med. Chem. 2003; 46:2413–2426. [PubMed: 12773045]

20. Sadhu C, Dick K, Tino WT, Staunton DE. Selective role of PI3Kd in neutrophil inflammatory responses. Biochem. Biophys. Res. Commun. 2003; 308:764–769. [PubMed: 12927784]

21. Murata T, Shimada M, Sakakibara S, Yoshino T, Masuda T, Shintani T, Sato H, Koriyama Y, Fukushima K, Nunami N, Yamauchi M, Fuchikami K, Komura H, Watanabe A, Ziegelbauer KB, Bacon KB, Lowinger TB. Synthesis and structure–activity relationships of novel IKK-β inhibitors. Part 3: Orally active anti-inflammatory agents. Bioorg. Med. Chem. Lett. 2004; 14:4019–4022. [PubMed: 15225718]

22. Pomel V, Klicic J, Covini D, Church DD, Shaw JP, Roulin K, Burgat-Charvillon F, Valognes D, Camps M, Chabert C, Gillieron C, Françon B, Perrin D, Leroy D, Gretener D, Nichols A, Vitte PA, Carboni S, Rommel C, Schwarz MK, Rückle T. Furan-2-ylmethylene thiazolidinediones as novel, potent, and selective inhibitors of phosphoinositide 3-kinase γ. J. Med. Chem. 2006; 49:3857–3871. [PubMed: 16789742]

23. Yaguchi S, Fukui Y, Koshimizu I, Yoshimi H, Matsuno T, Gouda H, Hirono S, Yamazaki K, Yamori T. Antitumor activity of ZSTK474, a new phosphatidylinositol 3-kinase inhibitor. J. Natl. Cancer Inst. 2006; 98:545–556. [PubMed: 16622124]

24. Kent LM, Smyth LJC, Plumb J, Clayton CL, Fox SM, Ray DW, Farrow SN, Singh D. Inhibition of lipopolysaccharide-stimulated chronic obstructive pulmonary disease macrophage inflammatory gene expression by dexamethasone and the p38 mitogen-activated protein kinase inhibitor *N*-cyano-*N*′-(2-{[8-(2,6-difluorophenyl)-4-(4-fluoro-2-methylphenyl)-7-oxo-7,8-dihydropyrido[2,3-*d*] pyrimidin-2-yl]amino}ethyl)guanidine (SB706504). J. Pharmacol. Exp. Ther. 2009; 328:458–468. [PubMed: 19004925]

25. Page TH, Brown A, Timms EM, Foxwell BMJ, Ray KP. Inhibitors of p38 suppress cytokine production in rheumatoid arthritis synovial membranes: Does variable inhibition of interleukin-6 production limit effectiveness in vivo? Arthritis Rheum. 2010; 62:3221–3231. [PubMed: 20589681]

26. Zhou L, Zuo Z, Chow MSS. Danshen: An overview of its chemistry, pharmacology, pharmacokinetics, and clinical use. J. Clin. Pharmacol. 2005; 45:1345–1359. [PubMed: 16291709]

27. Shi X, Huang L, Xiong S, Zhong X. Protective effect of tanshinone II A on lipopolysaccharide-induced lung injury in rats. Chin. J. Integr. Med. 2007; 13:137–140. [PubMed: 17609914]

28. Xu M, Dong MQ, Cao FL, Liu ML, Wang YX, Dong HY, Huang YF, Liu Y, Wang XB, Zhang B, Zhao PT, Luo Y, Niu W, Cui Y, Li ZC. Tanshinone IIA reduces lethality and acute lung injury in LPS-treated mice by inhibition of PLA2 activity. Eur. J. Pharmacol. 2009; 607:194–200. [PubMed: 19326571]

29. Elks PM, Eeden FJV, Dixon G, Wang X, Reyes-Aldasoro CC, Ingham PW, Whyte MKB, Walmsley SR, Renshaw SA. Activation of hypoxia-inducible factor-1 (Hif-1) delays inflammation resolution by reducing neutrophil apoptosis and reverse migration in a zebrafish inflammation model. Blood. 2011; 118:712–722. [PubMed: 21555741]

30. Lee A, Whyte MK, Haslett C. Inhibition of apoptosis and prolongation of neutrophil functional longevity by inflammatory mediators. J. Leukoc. Biol. 1993; 54:283–288. [PubMed: 8409750]

31. Matute-Bello G, Liles WC, Radella F, Steinberg KP, Ruzinski JT, Jonas M, Chi EY, Hudson LD, Martin TR. Neutrophil apoptosis in the acute respiratory distress syndrome. Am. J. Respir. Crit. Care Med. 1997; 156:1969–1977. [PubMed: 9412582]

32. Hannah S, Mecklenburgh K, Rahman I, Bellingan GJ, Greening A, Haslett C, Chilvers ER. Hypoxia prolongs neutrophil survival in vitro. FEBS Lett. 1995; 372:233–237. [PubMed: 7556675]

33. Savill JS, Wyllie AH, Henson JE, Walport MJ, Henson PM, Haslett C. Macrophage phagocytosis of aging neutrophils in inflammation. Programmed cell death in the neutrophil leads to its recognition by macrophages. J. Clin. Invest. 1989; 83:865–875. [PubMed: 2921324]

34. Yoo SK, Huttenlocher A. Spatiotemporal photolabeling of neutrophil trafficking during inflammation in live zebrafish. J. Leukoc. Biol. 2011; 89:661–667. [PubMed: 21248150]

35. Hall C, Flores MV, Storm T, Crosier K, Crosier P. The zebrafish lysozyme C promoter drives myeloid-specific expression in transgenic fish. BMC Dev. Biol. 2007; 7:42. [PubMed: 17477879]

36. Hughes J, Johnson RJ, Mooney A, Hugo C, Gordon K, Savill J. Neutrophil fate in experimental glomerular capillary injury in the rat. Emigration exceeds in situ clearance by apoptosis. Am. J. Pathol. 1997; 150:223–234. [PubMed: 9006338]

37. Cooke BM, Usami S, Perry I, Nash GB. A simplified method for culture of endothelial cells and analysis of adhesion of blood cells under conditions of flow. Microvasc. Res. 1993; 45:33–45. [PubMed: 8479340]

38. Holmes GR, Dixon G, Anderson SR, Reyes-Aldasoro CC, Elks PM, Billings SA, Whyte MKB, Kadirkamanathan V, Renshaw SA. Drift-diffusion analysis of neutrophil migration during inflammation resolution in a zebrafish model. Adv. Hematol. 2012; 2012:792163. [PubMed: 22899935]

39. Holmes GR, Anderson SR, Dixon G, Robertson AL, Reyes-Aldasoro CC, Billings SA, Renshaw SA, Kadirkamanathan V. Repelled from the wound, or randomly dispersed? Reverse migration behaviour of neutrophils characterized by dynamic modelling. J. R. Soc. Interface. 2012; 9:3229–3239. [PubMed: 22951343]

40. Toni T, Welch D, Strelkowa N, Ipsen A, Stumpf MPH. Approximate Bayesian computation scheme for parameter inference and model selection in dynamical systems. J. R. Soc. Interface. 2009; 6:187–202. [PubMed: 19205079]

41. Leitch AE, Riley NA, Sheldrake TA, Festa M, Fox S, Duffin R, Haslett C, Rossi AG. The cyclin-dependent kinase inhibitor R-roscovitine down-regulates Mcl-1 to override pro-inflammatory signalling and drive neutrophil apoptosis. Eur. J. Immunol. 2010; 40:1127–1138. [PubMed: 20127676]

42. Yin X, Yin Y, Cao F, Chen Y, Peng Y, Hou W, Sun S, Luo Z. Tanshinone IIA attenuates the inflammatory response and apoptosis after traumatic injury of the spinal cord in adult rats. PLOS One. 2012; 7:e38381. [PubMed: 22675554]

43. Tang C, Xue H, Bai C, Fu R. Regulation of adhesion molecules expression in TNF-α-stimulated brain microvascular endothelial cells by tanshinone IIA: Involvement of NF-κB and ROS generation. Phytother. Res. 2011; 25:376–380. [PubMed: 20687137]

44. Jeon SJ, Son KH, Kim YS, Choi YH, Kim HP. Inhibition of prostaglandin and nitric oxide production in lipopolysaccharide-treated RAW 264.7 cells by tanshinones from the roots of *Salvia miltiorrhiza* bunge. Arch. Pharm. Res. 2008; 31:758–763. [PubMed: 18563358]

45. Jang SI, Kim HJ, Kim Y, Jeong S, You Y. Tanshinone IIA inhibits LPS-induced NF-κB activation in RAW 264.7 cells: Possible involvement of the NIK–IKK, ERK1/2, p38 and JNK pathways. Eur. J. Pharmacol. 2006; 542:1–7. [PubMed: 16797002]

46. Kogut MH, Genovese KJ, He H, Kaiser P. Flagellin and lipopolysaccharide up-regulation of IL-6 and CXCLi2 gene expression in chicken heterophils is mediated by ERK1/2-dependent activation of AP-1 and NF-κB signaling pathways. Innate Immun. 2008; 14:213–222. [PubMed: 18669607]

47. Yang C, Luo S, Hsieh H, Chi P, Lin C, Wu C, Hsiao L. Interleukin-1β induces ICAM-1 expression enhancing leukocyte adhesion in human rheumatoid arthritis synovial fibroblasts: Involvement of ERK, JNK, AP-1, and NF-κB. J. Cell. Physiol. 2010; 224:516–526. [PubMed: 20432452]

48. Hallett JM, Leitch AE, Riley NA, Duffin R, Haslett C, Rossi AG. Novel pharmacological strategies for driving inflammatory cell apoptosis and enhancing the resolution of inflammation. Trends Pharmacol. Sci. 2008; 29:250–257. [PubMed: 18407359]

49. Burgon J, Robertson AL, Hoggett EE, Ward JR, Wang X, Farrow SN, Zuercher WJ, Ingham PW, Hurlstone AF, Whyte MKB, Renshaw SA. Serum and glucocorticoid regulated kinase 1 (SGK1) regulates neutrophil clearance during inflammation resolution. J. Immunol. 2014; 192:1796–1805. [PubMed: 24431232]

50. Hamza B, Wong EA, Patel S, Cho H, Martel J, Irimia D. Retrotaxis of human neutrophils during mechanical confinement inside microfluidic channels. Integr. Biol. 2014; 6:175–183.

51. Nüsslein-Volhard, C.; Dahm, R. A Practical Approach. ed. 1. Oxford: Oxford Univ. Press; 2002. Zebrafish.

52. Wardle DJ, Burgon J, Sabroe I, Bingle CD, Whyte MKB, Renshaw SA. Effective caspase inhibition blocks neutrophil apoptosis and reveals Mcl-1 as both a regulator and a target of neutrophil caspase activation. PLOS One. 2011; 6:e15768. [PubMed: 21253591]
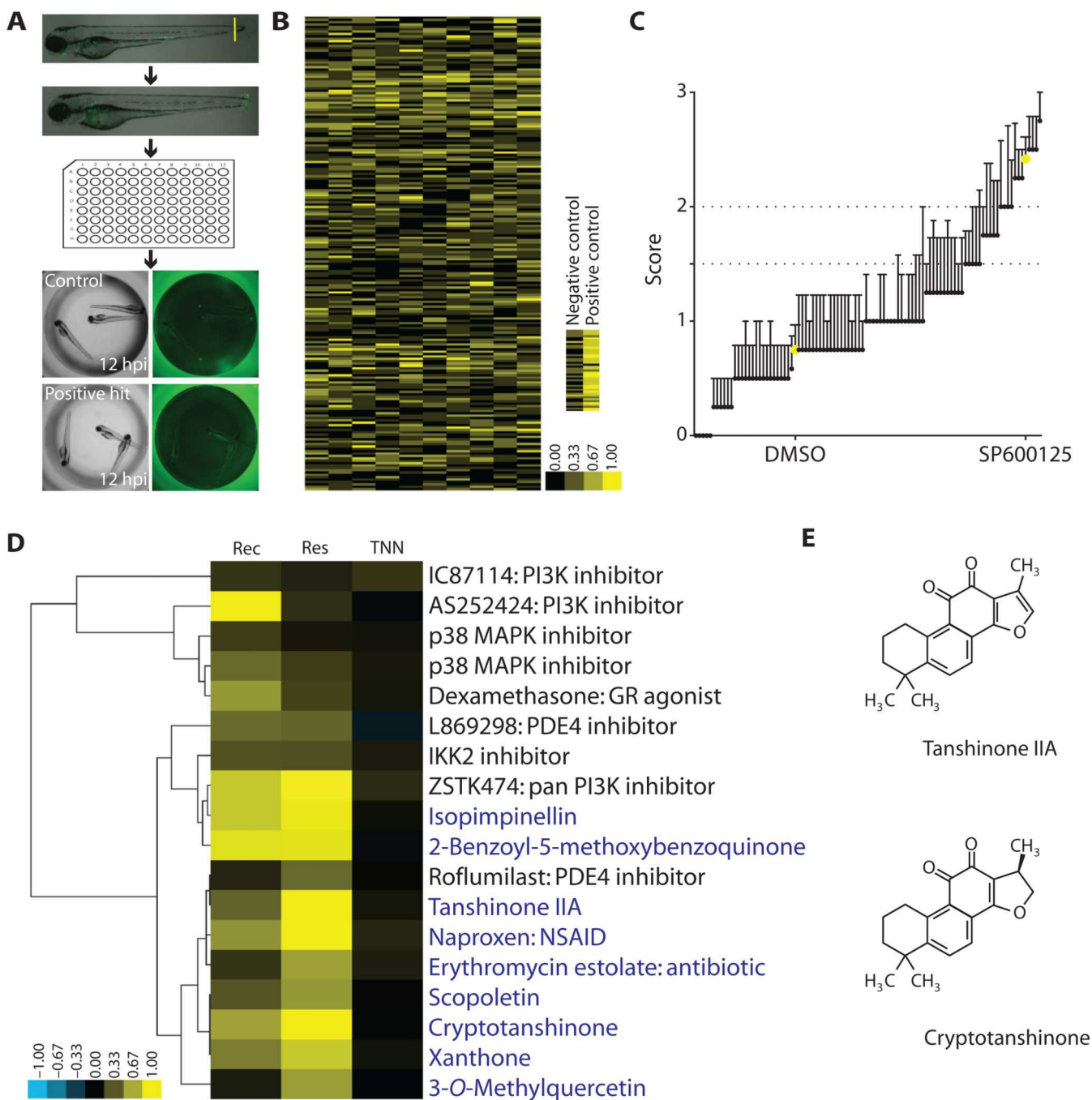
Fig. 1. An in vivo chemical genetic screen identifies compounds with specific proresolution activity

(**A**) Injured 3 dpf *mpx*:GFP larvae were treated with screening compounds at 4 hpi. Plates were imaged at 12 hpi and analyzed by manual scoring. Lower panel: Representative DMSO vehicle control well and a positive hit compound. (**B**) Heat map represents mean scores of all 2000 compounds from the primary screen of the Spectrum Collection (*n* = 6). Right panel: Representative scores of the negative control (1% DMSO) and positive control (30 μM SP600125). (**C**) The initial 95 hits, scoring 1.5 in the primary screen, were rescreened.

Graph shows mean scores ± SEM ($n = 12$). Dotted line at $y = 1.5$ indicates threshold for positive hit selection. Hits scoring 2 (as indicated) were selected for further testing. (**D**) Clustergram represents secondary assay data for hit compounds (named in blue) and existing tool compounds (named in black). Increased yellow intensity indicates reduction in neutrophil number. Doses shown are 1 μM erythromycin estolate, 10 μM cryptotanshinone and 2-benzoyl-methoxybenzoquinone, and 25 μM for all other compounds. (**E**) Tanshinone IIA and cryptotanshinone shared close structural similarity.
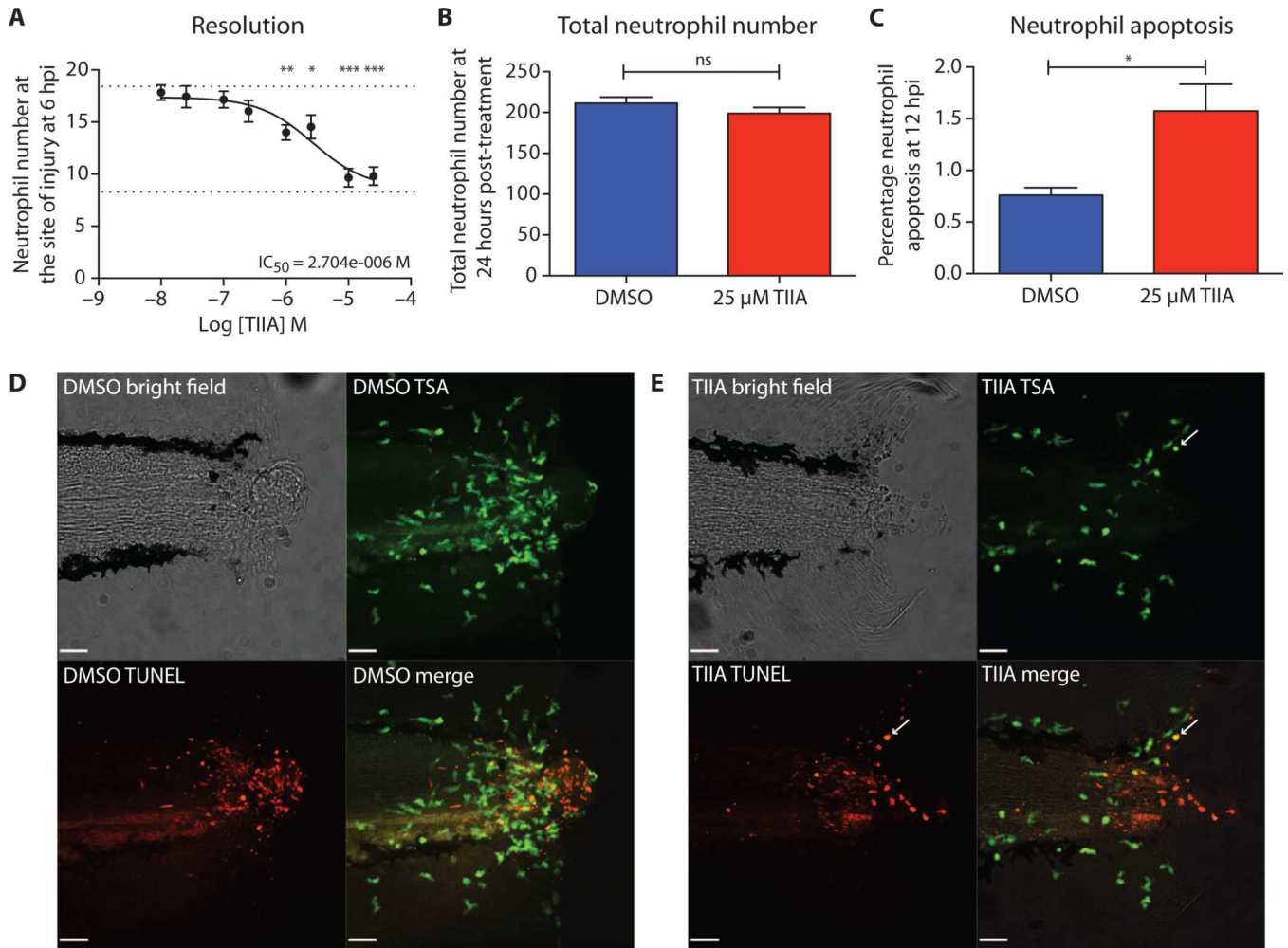
Fig. 2. Tanshinone IIA accelerates resolution of neutrophilic inflammation in vivo
(**A**) Larvae were injured and treated from 6 hpi with varying doses of tanshinone IIA (TIIA). Neutrophil numbers at the wound were counted at 12 hpi [one-way analysis of variance (ANOVA) with Dunnett' s multiple comparison post-test, $^*P < 0.05$, $^{**}P < 0.01$, and $^{***}P < 0.001$; $n = 24$, performed as four independent experiments]. Dotted lines at $y = 18.42$ and $y = 8.28$ indicate mean neutrophil numbers in DMSO control larvae and representative 30 μM SP600125–treated larvae, respectively. (**B**) Larvae were incubated with 25 μM tanshinone IIA or DMSO for 24 hours and imaged, and total neutrophil numbers were analyzed with ImageJ (unpaired t test, $P = 0.242$ (ns, not significant); $n = 18$ performed as three independent experiments). (**C**) After the resolution assay, larvae were fixed at 12 hpi for tyramide signal amplification (TSA)/terminal deoxynucleotidyl transferase–mediated deoxyuridine triphosphate nick end labeling (TUNEL) staining and imaging. Numbers of TSA-positive neutrophils and TSA/TUNEL double-positive apoptotic neutrophils at the wound were counted to calculate percentage apoptosis (unpaired t test, $P = 0.0206$; $n   161$, performed as three independent experiments). (**D** and **E**) Representative images of (D) DMSO-treated and (**E**) 25 μM tanshinone IIA–treated larvae after TSA/TUNEL staining. White arrows in (E) indicate apoptotic neutrophil, identified by condensed, rounded

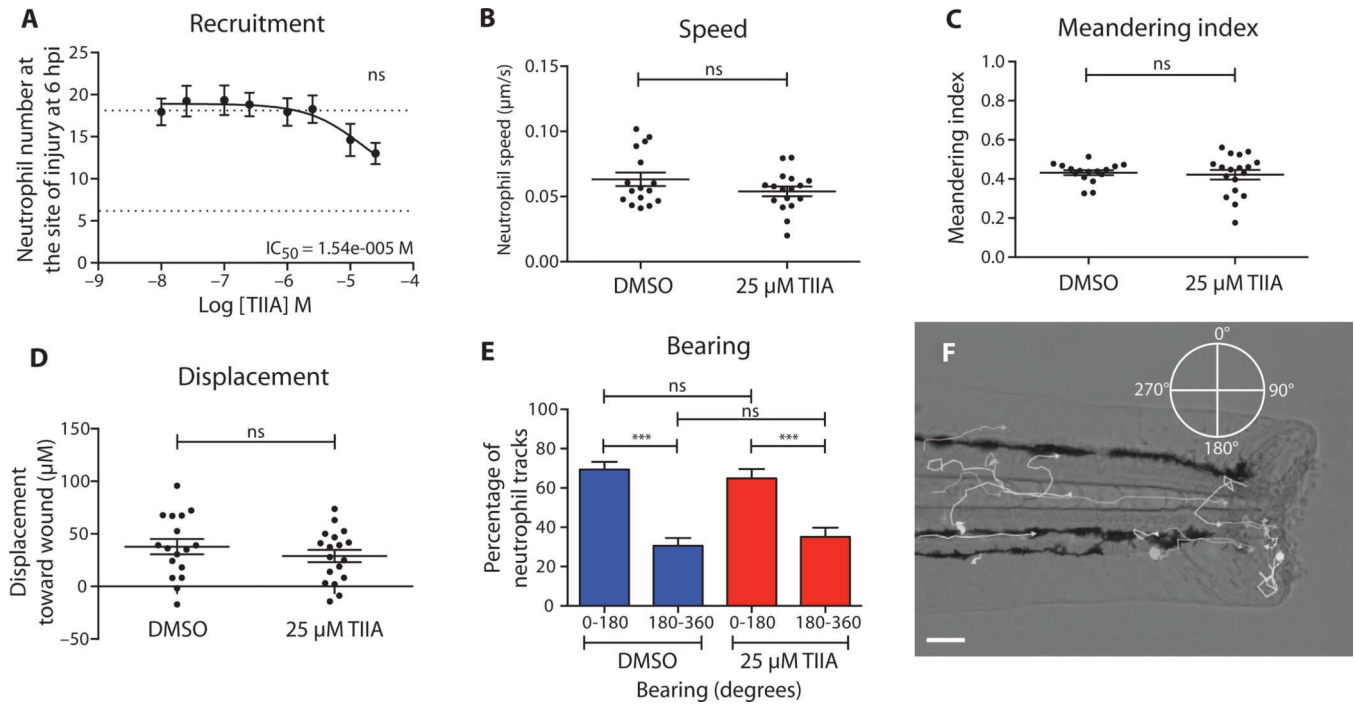morphology and double TSA/TUNEL labeling. Scale bars, 70 μm. In all graphs, data are means from each larva ± SEM.

Fig. 3. Tanshinone IIA does not significantly affect neutrophil recruitment

(**A**) Larvae were injured and treated immediately with varying doses of tanshinone IIA (TIIA). Neutrophil numbers at the wound were counted at 6 hpi (one-way ANOVA with Dunnett's multiple comparison post-test; $n = 18$, performed as three independent experiments). Dotted lines at $y = 18.11$ and $y = 6.22$ indicate mean neutrophil numbers in DMSO control larvae and representative 30 μM SP600125–treated larvae, respectively. (**B** to **F**) Larvae were pretreated with either DMSO or 25 μM tanshinone IIA for 2 hours before injury and imaging. Individual GFP-labeled neutrophils were tracked and analyzed with Volocity software to compare (B) neutrophil speed, (C) meandering index, and (D) displacement toward the wound (unpaired t test, $P = 0.331$ for meandering index and $P = 0.348$ for displacement; $n = 18$, performed as three independent experiments). For bearing (E), an angle of 0 to 180° indicates movement toward the wound and an angle of 180 to 360° indicates movement away (one-way ANOVA with Bonferroni's multiple comparison post-test to compare selected columns, $P < 0.001$; $n = 18$, performed as three independent experiments). (F) Representative example of neutrophil tracks during recruitment. Scale bar, 60 μm. In all graphs, data are means from each larva ± SEM.
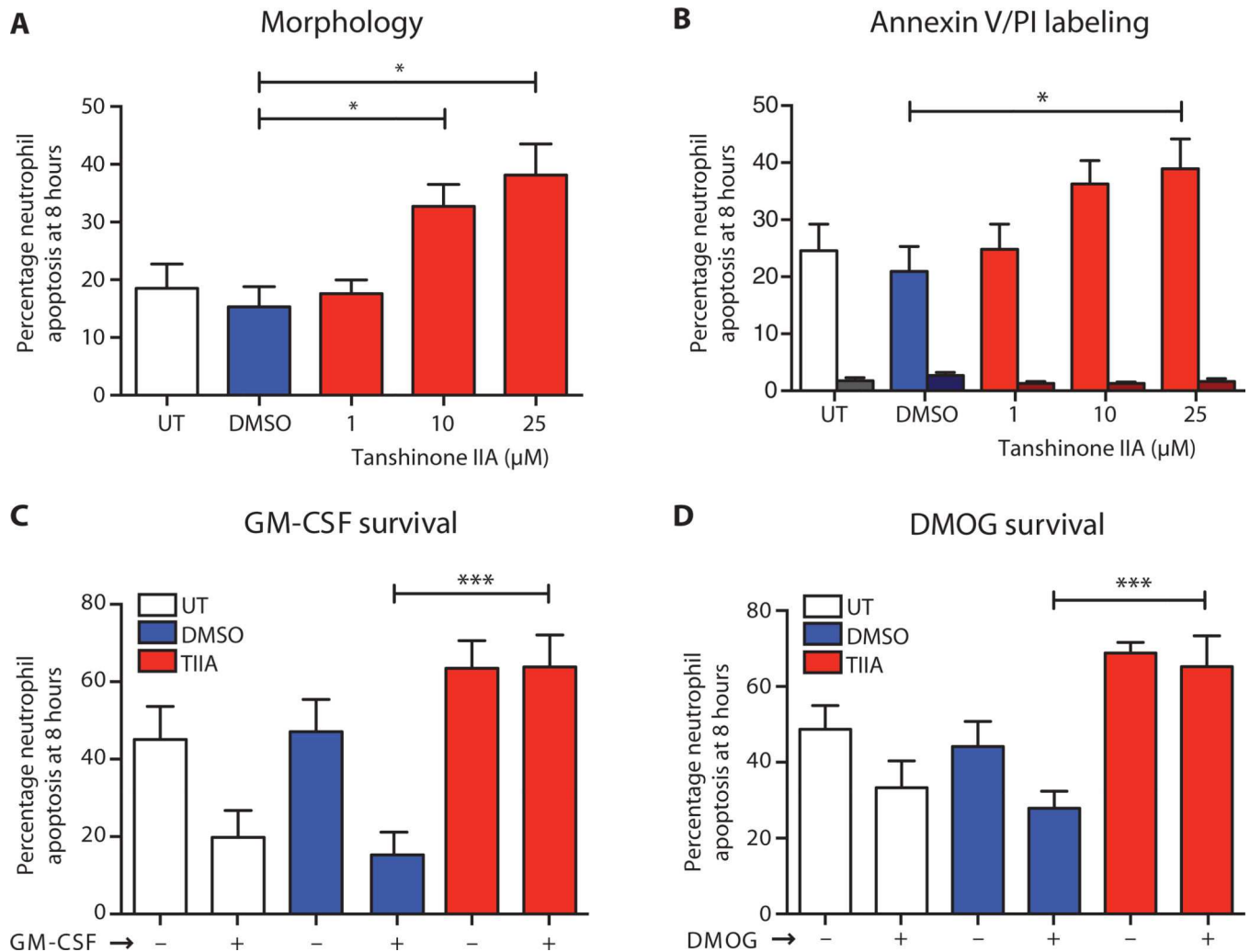
Fig. 4. Tanshinone IIA accelerates neutrophil apoptosis in vitro and overrides survival signaling
(**A** to **D**) Isolated human neutrophils were incubated with DMSO or tanshinone IIA (TIIA) at the dose indicated for 8 hours at 37°C. For each condition, percentage neutrophil apoptosis was calculated from assessment of duplicate cytospins on the basis of nuclear morphology. Untreated neutrophils (UT) and neutrophils treated with DMSO as a vehicle control were used as controls to compare the effects of tanshinone IIA on apoptosis of (A) unstimulated neutrophils (one-way ANOVA with Dunnett's multiple comparison post-test, $P < 0.05$; $n = 4$) and neutrophils incubated with (+) or without (−) (C)GM-CSF (0.01 μg/ml) or (D) 100 μM DMOG (one-way ANOVA with Bonferroni's multiple comparison post-test, $P < 0.001$; $n = 3$). Neutrophil apoptosis was also assessed by flow cytometry after annexin V/PI labeling (B). Samples were run in duplicate, and 10,000 events were captured within the neutrophil gate each time. Lighter bars (on the left of each condition) represent annexin V–positive/PI-negative neutrophils, and darker bars (on the right) represent annexin V–positive/PI-positive neutrophils (one-way ANOVA with Dunnett's multiple comparison post-test, $P < 0.05$; $n = 3$). In all graphs, error bars represent SEM.
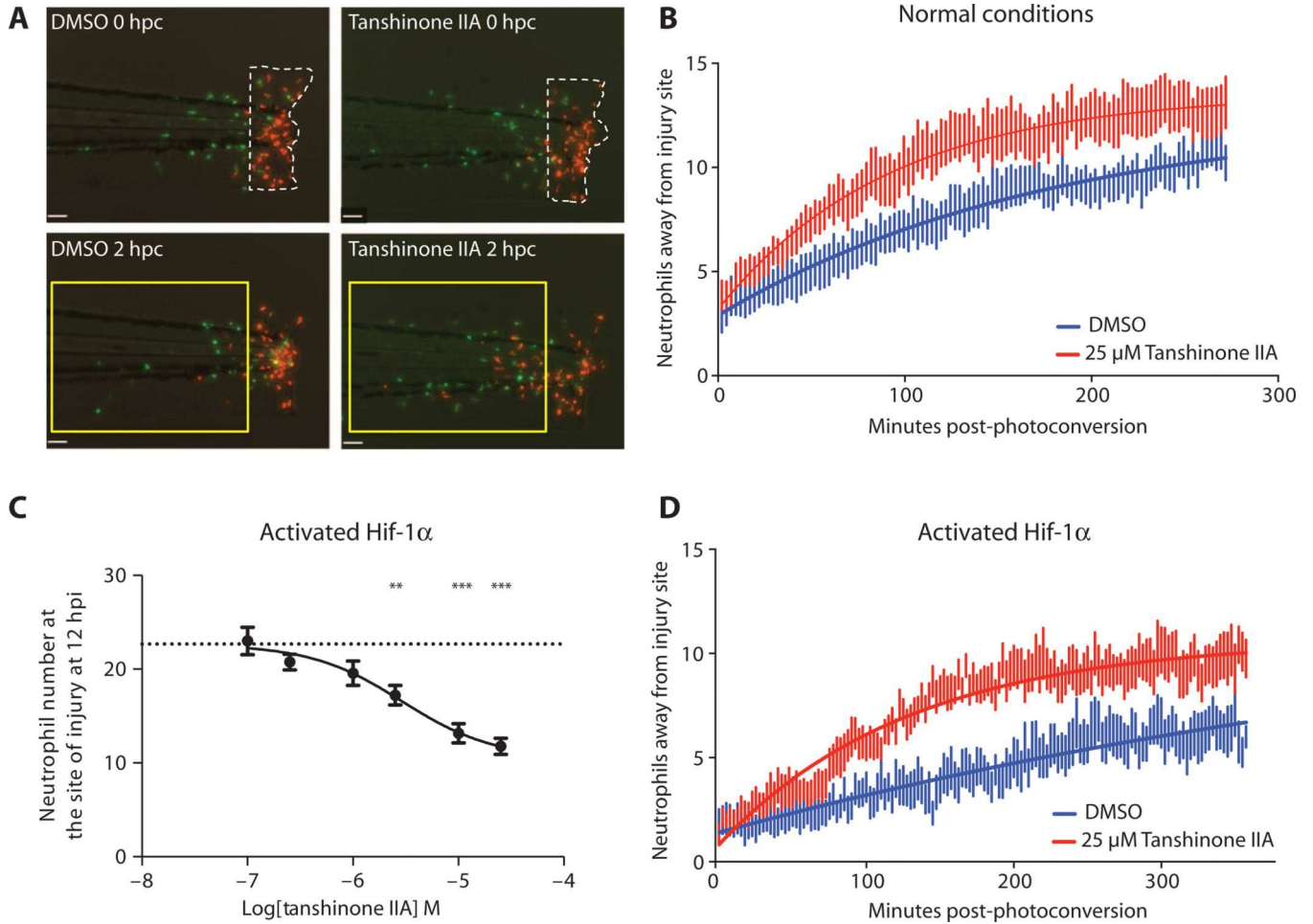
Fig. 5. Tanshinone IIA accelerates resolution of inflammation in vivo by promoting reverse migration of neutrophils away from the site of injury

(**A**, **B**, and **D**) Tail transection was performed on *mpx*/Kaede larvae followed by treatment with either DMSO or 25 μM tanshinone IIA at 4 hpi, photoconversion of neutrophils at the wound at 6 hpi, and time-lapse imaging. (A) Representative images of DMSO- and tanshinone IIA–treated larvae at 0 and 2 hours post-photoconversion (hpc). Dotted line indicates photoconverted region, and yellow box indicates region in which neutrophil numbers were quantified. Scale bars, 60 μm. (B) Larvae were imaged, and the number of red fluorescent cells that migrated away from the wound into the defined region was quantified over the time course (*n* = 24, performed as four independent experiments). (**C**) At the one-cell stage, *mpx*:GFP embryos were injected with 100 ng of dominant-active *hif-1αb* RNA. At 2 dpf, larvae were injured and treated with either DMSO or 25 μM tanshinone IIA at 6 hpi, and neutrophil numbers at the wound were counted at 12 hpi (one-way ANOVA with Dunnett's multiple comparison post-test, **$P < 0.01$ and ***$P < 0.001$; *n* = 18, performed as three independent experiments). (D) As described for (A) and (B), reverse migration assays were performed at 2 dpf in *mpx*/Kaede larvae injected with 100 ng of dominant-active *hif-1αb* RNA at the one-cell stage (*n* = 18, performed as three independent experiments). In all graphs, data are means ± SEM.
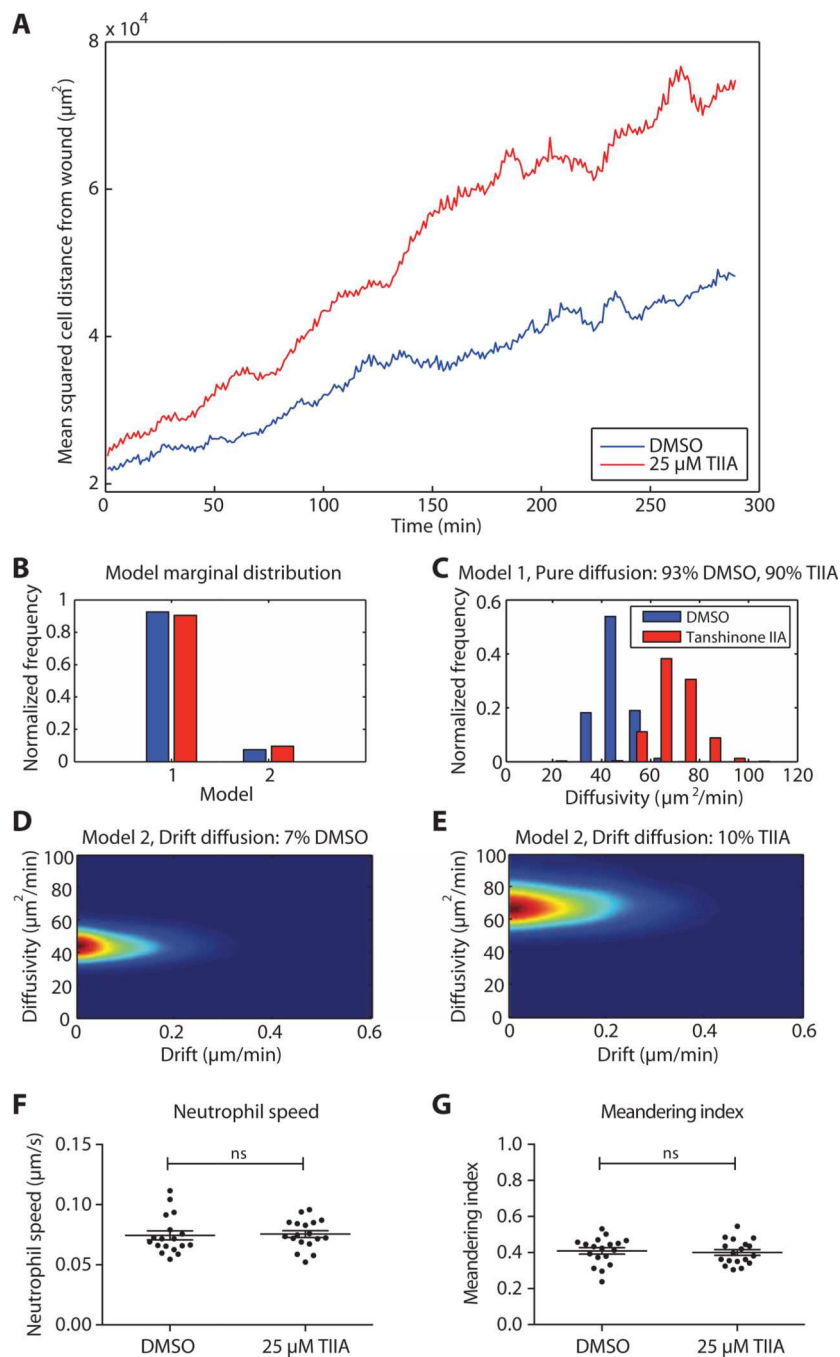
Fig. 6. Tanshinone IIA promotes neutrophil reverse migration by nondirectional redistribution rather than active fugetaxis

(**A** to **E**) Data analysis was performed as described (38, 39), using the data presented in Fig. 5B (*n* = 24, performed as four independent experiments). (A) The coordinates of each neutrophil centroid were identified in Volocity and used to calculate the mean squared distance from the wound over time in larvae treated with DMSO or 25 μM tanshinone IIA. Data represent about 25 neutrophils from each larva (total of about 600 neutrophils per condition). (B to E) Simulation-based approximate Bayesian computation–sequential Monte

Carlo (ABC-SMC) modeling (39) was applied to analyze neutrophil reverse migration and select the best candidate model from either pure diffusion (model 1) or drift diffusion (model 2). (**F** and **G**) Neutrophil tracks were analyzed with Volocity to measure the (F) neutrophil speed and (G) meandering index of reverse migrating neutrophils (unpaired *t* test, $P = 0.8196$ for speed and $P = 0.7244$ for meandering index; $n = 18$, performed as three independent experiments; data are means from each larva ± SEM).